Quantifying the Impact of Synaptic Delay and Neuronal Refractory Period on Criticality in Hierarchical Modular Neural Networks

Hannes Gustafsson

***Abstract*—Self-organized brain criticality suggests that the brain is able to operate near a critical point. With compelling evidence supporting the theory, it is important to understand which biological mechanisms are required for critical dynamics to occur. Previous studies have investigated the relation between network structure and brain criticality an shown promising results. However, most overlook a crucial aspect of networks with limited size: the relation between synaptic delay and neuronal refractory period.**

The aim of this project is to quantify the impact of synaptic delay and neuronal refractory period in hierarchical modular neural networks (HMN). The results showed that both variables had a significant impact on the characteristics of neuronal avalanches, which is an phenomena of critical dynamics.

However, the analysis indicates the it is only the synaptic delay that has a significant impact on critical dynamics as the impact of neuronal refractory period vanished. To conclude, further studies using HMN to investigate criticality should not overlook the impact synaptic delay has on the results.

***Sammanfattning*—Själv-organiserad hjärnkritikalitet är en hypotes postulerar att hjärnan kan organisera sig själv nära en kritisk punkt. Med övertygande bevis som stödjer hypotesen, är det viktigt att förstå vilka biologiska mekanismer som krävs för att kritikalitet i hjärnan ska uppstå. Tidigare studier har undersökt sambandet mellan nätverksstruktur och hjärnkritikalitet med lovande resultat. Men de flesta förbiser en avgörande aspekt av nätverk med begränsad storlek: förhållandet mellan synaptisk fördröjning och neuronal återhämtningsperiod.**

Syftet med detta projekt är att kvantifiera effekten av synaptisk fördröjning och neuronal återhämtningsperiod i hierarkiska modulära neurala nätverk (HMN). Resultaten visade att båda variablerna hade en signifikant inverkan på egenskaperna hos neuronala laviner, vilket är ett fenomen av kritisk dynamik.

Analysen indikerar dock att det bara är den synaptiska fördröjningen som har en betydande inverkan på kritisk dynamik när effekten av den neuronala refraktärperioden försvann. Sammanfattningsvis bör ytterligare studier som använder HMN för att undersöka kritikalitet inte förbise effekten av synaptisk fördröjning på resultaten.

***Index Terms*—Hierarchical Modular Neural Networks, Synaptic Delay, Neuronal Refractory Period, Criticality, Neuronal Avalanches**

Supervisor: Pawel Herman

TRITA number:

I. Introduction

The human brain is one of the most complex systems known to science, with billions of neurons connected through intricate networks of synapses [1]. Despite this seemingly chaotic complexity, we know from introspection that we experience seemingly ordered macroscopic phenomena such as consciousness, information processing, and reasoning capabilities in our everyday lives. Within the field of neuroscience, this must be understood as emerging from the underlying neuronal collective.

Self-organized criticality (SOC) has been proposed as a possible explanation for the brain's ability to operate near a critical point between order and disorder, known as the critical brain hypothesis. This hypothesis suggests that the brain operates near a critical point in order to achieve a balance between stability and adaptability, and that this critical state may be important for many cognitive processes, including perception, memory, and decision-making [2]. In 2003, Beggs and Plenz presented the first compelling evidence of this by examining slices of rat cortex that neuronal populations can display critical dynamics [3]. Since then, experiments have found more signs of criticality in rats [4], monkeys [5], and human brains [6].

Understanding which biological mechanisms are required for critical dynamics to occur in the brain has become a important research question. It has been shown that criticality critical dynamics can arise from networks short-term synaptic plasticity [7], dynamical synapses [8] and an adaptive firing threshold [9]. Apart from cellular mechanism, functionality is also known to emerge from the brain exhibiting a complex network structure. For example, in the cortical area of the brain neurons are grouped into modules with functional roles that are connected hierarchically with higher-level modules regulating the activity of lower-level modules [10] [11]. It is therefore important to also understand the relation between criticality and network structure.

When studying criticality in hierarchical modular networks (HMN) it is important to carefully consider the relation between synaptic delay and neuronal refractory period. If a network of sufficiently small size exhibits just the right configuration of synaptic delay and neuronal refractory period, it could happen that network activity dies out simply because no neuron had time to recover. This is also motivated from a biological view, since the cortical brain area is known to have wide range of synaptic delays [12]. Implying that there is a non-zero probability of one such configuration occurring.

However, this relation is typically overlooked by most research on this topic. One study that investigated different connectivity patterns of HMN initialized the synaptic delays uniformly between 1 and 10 ms [13] with a refractory period of 3 ms, while another study that investigated the impact of

HMN on critical robustness, initialized the refractory period to 5 ms but left the synaptic delay at 0 ms [14]. Another study set the refractory period to 0 ms [15].

A. Research question

The aim of this project is thus to quantify the robustness of critical dynamics in cortical brain networks with respect to synaptic delay and the neuronal refractory period. In particular, we seek to answer the following question:

1) *Does synaptic delay and neuronal refractory period have a significant impact on criticality in hierarchical modular neural networks?*
2) *If so, what kind of impact?*

II. Theory and Background

A. The Spiking Neuron Model

The spiking neuron model is a mathematical framework that describes how neurons generate and transmit electrical signals, known as spikes. It is based on the idea that neurons change their membrane potential in response to incoming signals, and when the potential reaches a certain threshold, an action potential is triggered, leading to the release of neurotransmitters and communication with other neurons [16].

The leaky integrate and fire (LIF) model is a simplified spiking neuron model that describes how neurons generate and transmit electrical signals. In the LIF model, the neuron's membrane potential is represented as a continuous variable that changes over time in response to incoming signals. However, the membrane potential gradually leaks away over time, leading to a decay in the signal, see Figure 1 [16].

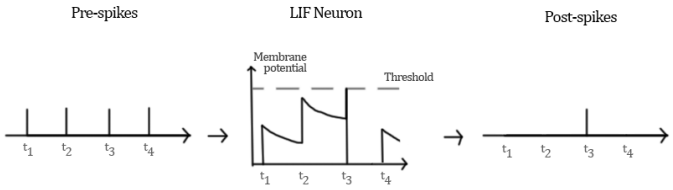

Fig. 1. An illustration of the leaky integrate-and-fire neuron membrane dynamics. Notice how the spikes at t_1 and t_2 would have been sufficient for the membrane potential to cross the threshold in absence of the leak.

B. E/I Tuning and The Balanced Region

Excitatory neurons are a type of nerve cell that transmit signals to other neurons by releasing neurotransmitters that increase the likelihood of an action potential. Inhibitory neurons, on the other hand, also transmit signals to other neurons, but by releasing neurotransmitters that decrease the likelihood of an action potential [17].

E/I tuning in neuronal networks refers to the balance between excitatory and inhibitory input received by neurons in the network. This balance is critical for proper neuronal function, as an excessive level of excitation can lead to overexcitation, while an excessive level of inhibition can lead to reduced neuronal activity [18].

Here, balance between excitation and inhibition is regulated by tuning the synaptic strengths ($\Delta g_{inh}, \Delta g_{ex}$) of excitatory and inhibitory neurons. Figure 2 shows the result of systematically stimulating the network for 200 ms, then removing the stimulation and measuring how long the activity sustains for different parameters ($\Delta g_{inh}, \Delta g_{ex}$). The figure is adapted from Figure 2 in [14] and Figure 1 in [19] since their network models are structure similar to the one used here.

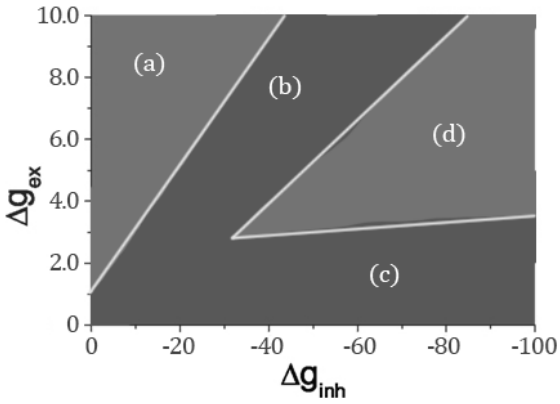

Fig. 2. The network displays different dynamics depending on the synaptic tuning. $R_{ex} = 0.99$, $R_{inh} = 1$, N=10 000, $P_0 = 1$. In regions (b) and (c), network activity dies out once stimulation is removed. For region (a), excitatory neurons dominate causing the network to be overactive. Region (d) yields a balanced network where activity sustains, without going into overactivity. The figure is adapted from Figure 2 in [14] and Figure 1 in [19].

C. Synaptic delay and neuronal refractory period

The first parameter of interest in this report is the *synaptic delay*. Here, we will use it to refer to the time it takes for an action potential to travel down the length of an axon on a neuron and active the postsynaptic receptors. This delay is determined by several factors, including the axon's length, diameter, and the presence of insulating layers that wrap around the axon and can increase the speed of conduction [20]. Within the cortex, synaptic axon delays are empirically estimated to range between 1ms - 10 ms [12].

The other parameter of interest is the neuronal refractory period, which is the refractory period in a neuron that occurs after the neuron has fired an action potential. It generally lasts 1-2 ms [21], but values up to 5 ms has been used in computational simulations [14] [19].

D. Classifying Self-organized Criticality

Self-organized criticality is characterized by the spontaneous formation of a so called critical state, where small perturbations can lead to large-scale changes in the system without causing it to collapse or become unstable [22]. A wide range of phenomena, such as swarm models [23], forest fires [24], and the financial market [25] have been found exhibiting criticality. But how is a system classified as critical?

The signature of a critical system is its scale-invariant dynamics where short-range interactions can cause long-range correlated patterns to emerge. For neuronal populations, this

manifests itself in that an initial spike of activity can sometimes generate a cascade of subsequent activity spreading throughout the network called *neuronal avalanches*.

If a system is critical, then the duration and size of the neuronal avalanches would follow a power-law distribution (which has the property of scale-invariance) [2]:

$$\text{avalanche size} \propto x^{-\beta} \tag{1}$$

$$\text{avalanche duration} \propto x^{-\kappa}. \tag{2}$$

Theoretically, it has been shown that for a critical system we would expect $\beta = 2$ and $\kappa = 1.5$ [26].

However, experiments have shown that power-law distributed avalanches can occur in random systems that are not critical. This happens because the avalanche size and duration are correlated [27]. Therefore, one can also look at the power-law distribution of avalanche sizes *to* avalanche durations, called *avalanche shapes*. For neuronal avalanches, the critical exponent of avalanche shapes γ has been shown to be related to β and κ [28] as per

$$\gamma = \frac{\kappa - 1}{\beta - 1}. \tag{3}$$

From the theoretical values of β and κ, it follows that $\gamma = 2$.

III. Method

A. Model

We studied a network of N leaky integrate-and-fire neurons connected as hierarchical modules using a conductance-based model of neurons, and is based on a model from a previous study [14] on HMN. The ratio of excitatory and inhibitory neurons in the network is taken as 4:1. The dynamics of the membrane potential V evolve according to

$$\tau \frac{dV}{dt} = (V_{rest} - V) + g_{ex}(E_{ex} - V) + g_{inh}(E_{inh} - V). \tag{4}$$

When V exceeds the membrane potential threshold -50 mV, the neuron is said to spike and V is reset to V_{rest} = -60 mV for a τ_{ref} ms refractory period. The value of the time constant is τ = 20 ms and the reversal potentials of synapses for excitatory and inhibitory neurons are set to E_{ex} = 0 mV and E_{inh} = -80 mV, respectively. The synaptic conductances g_{ex} and g_{inh} are expressed in units of the resting membrane conductance, which is set to 1/(100 MΩ).

Neurons in the network are either excitatory or inhibitory. When a neuron fires, the appropriate synaptic variables of its postsynaptic targets are increased, $g_{ex} \to g_{ex} + \Delta g_{ex}$ for an excitatory presynaptic neuron and $g_{inh} \to g_{inh} + \Delta g_{inh}$ for an inhibitory presynaptic neuron. Theses parameters evolve according to:

$$\tau_{ex} \frac{dg_{ex}}{dt} = -g_{ex} \tag{5}$$

$$\tau_{inh} \frac{dg_{inh}}{dt} = -g_{inh}. \tag{6}$$

The synaptic time constants are set to τ_{ex} = 5 ms and τ_{inh} = 10 ms. The simulation step size was set to 0.1 ms.

B. Generating the Hierarchical Modular Network

The hierarchical modular network (HMN) is generated by rewiring a random network with a sparse connection probability P_0 in a top-down way, as proposed in both [14] and [15]. The network is randomly split into two subgroups i and j, called *modules*. Then, with probability R a synapse that is connected across the modules $(i \to j)$ is cut and rewired back into a randomly selected neuron within the source module $(i \to i)$. This yields a 1-level modular network. To generate a 2-level modular network, we recursively apply the rewiring process on each module. For a l-level network, the number of modules is m = 2^l.

The probabilities of rewiring for excitatory and inhibitory synapses are denoted R_{ex} and R_{inh}, respectively. As highlighted in the original paper [14], inhibitory connections are empirically known to be formed by local connections while excitatory connections can be both local or long-distance [29] [30]. Hence, we set R_{inh} = 1 and R_{ex} as a value in (0, 1). Figure 3 visualize the connection density between each module when N = 10 000, P = 0.01, R_{ex} = 0.99, and R_{inh} = 1, which are the parameter values that will be used throughout this report if not mentioned otherwise.

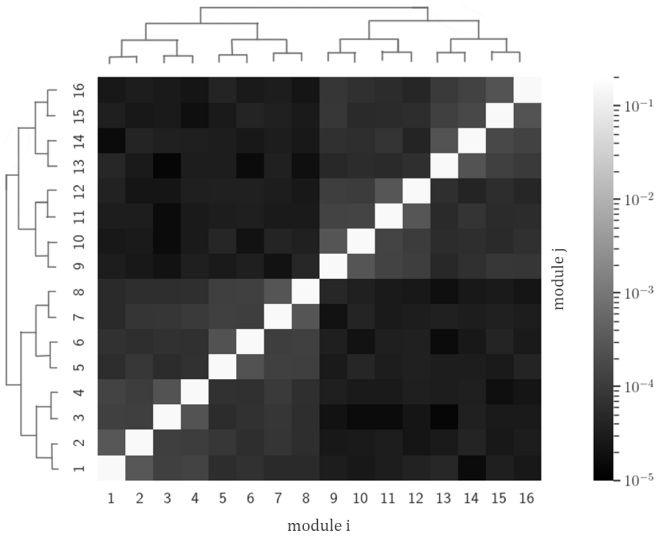

Fig. 3. The connection density matrix between the modules of a Hierarchical Modular Network (HMN). N = 10 000, p = 0.01, R_{ex} = 0.99, R_{inh} = 1. The connection densities are defined as the ratio of the number of connections to the possible number of connections. The hierarchy to the left and top sides of the heatmap denotes the module's hierarchical structure.

However, the number of synapses to the number of neurons N grows as $\mathcal{O}(N^2)$. Generating the HMN by recursively cutting and rewiring synapses quickly becomes computationally expensive. Instead, we utilize the analytically derived formulas for the connection probability within and across modules from the original paper [14]. The connection density within a module is

$$P_{within} = 0.8P_0(1 + R_{ex})^4 + 0.2P_0 2^4. \tag{7}$$

where the first term represents the connection probability of excitatory neurons, conditioned on the number of excitatory

neurons; the second term for inhibitory neurons. The connection density across two modules of the *i*-level is

$$P_{across} = 0.8P_0(1 + R_{ex})^{i-1}(1 - R_{ex}). \tag{8}$$

C. Input Stimulation

The robustness of the network was addressed by stimulating it with two types of input signals: background noise and external stimulation.

1) Background noise: To account for background noise within the brain, each neuron receives a piecewise constant current with a Gaussian-distributed amplitude given by

$$I(t) = \mu + N_j\sigma, \text{ for } j\delta < t < (j+1)\delta \tag{9}$$

where N_j are drawn from the unit normal distribution and δ the interval length. All neurons receive currents based on different samples of N_j. We set μ = 0 pA, σ = 50 pA, and δ = 10 ms had an effect when combined with external stimulation without dominating the network activity.

2) External stimulation: To model the network receiving signals from other areas of the brain, we generate input spikes using Poisson process statistics. The spike trains have exponentially distributed interspike intervals with a configurable mean firing rate λ (spikes / s).

The input spikes are generated with $\lambda = 5$ Hz and fed into modules 3, 6, 9, and 16 (see Figure 3). The module IDs were chosen so that the stimulation of the network respects the symmetry of the hierarchy. If one were to truncate the lowest level, the stimulus would still be symmetrical. In this way, no side dominates when averaging over time.

The Poison process generates unique spike trains for each of its targets.

D. Data Post-Processing

In order to quantify the effect of synaptic delay, we record the *spike trains* per module of each simulation: that is, the number of spikes per neuron at each time step for each module. The spike train was then processed as follows:

1) *Quantify the neuronal avalanches*: We compute frequency tables of three avalanche metrics: [1] avalanche distributions, [2] silent periods, and [3] avalanche sizes. As seen in Figure 4, an avalanche is defined as a sequence of continuous neuron firings. It begins when at least one neuron fires and ends at the first time step without any neurons firing. Avalanche size is the total number of neuron spikes during an avalanche.

   Although the simulation step is 0.1 ms, in the context of classifying avalanches a time step is defined as 1 ms - the shortest timescale across our simulation parameters. The frequency tables per module were then summed to obtain a frequency table per metric for the entire network.

2) *Estimate power-law coefficients*: Our aim now is to figure out whether these metrics follow a power-law distribution. To do this, we first estimate the metric probability distributions by normalizing the frequency tables. We then fit the probability distributions to a power-law distribution of the form $p(x;\ C_0, \alpha) = C_0 x^{-\alpha}$ using the Levenberg–Marquardt algorithm implemented by the `scipy.optimize.curve_fit` function in SciPy [31]. We now have a power-law coefficient α which encompasses the characteristics of each avalanche metric as a function of the synaptic delay τ_d and neuron refractory period τ_r.

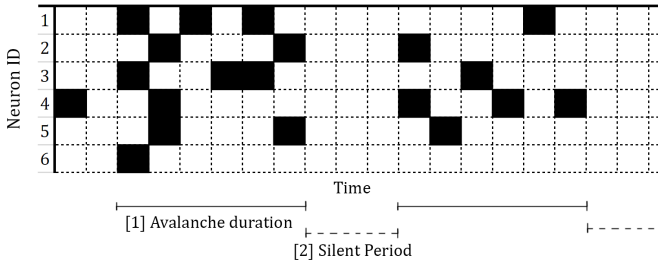

Fig. 4. Spike raster of a module with 6 neurons illustrating the definition of *avalanche duration* and *silent duration*. If a neuron spikes during a time step, it is denoted by a black square. Here, the avalanche duration is 6 time steps and the silent period is 3 time steps.

3) *Quantify the impact of synaptic delay and neuron refractory period*: Finally, we now want to conclude if synaptic delay and neuron refractory period has a significant effect on neuronal avalanches. We do this by constructing a multivariate polynomial of degree two $\hat{\alpha}(\tau_r, \tau_d)$, fitting the $\alpha(\tau_r, \tau_d)$ data and quantifying the significance of the coefficients $\{\beta_i\}$. That is,

$$\begin{aligned}\hat{\alpha}(\tau_d, \tau_r;\ \{\beta_i\}) = \beta_0 + \beta_1\tau_d + \beta_2\tau_r + \beta_3\tau_d^2 \\ + \beta_4\tau_d\tau_r + \beta_5\tau_r^2\end{aligned} \tag{10}$$

   The model parameters are estimated using Ordinary Least Square (OLS) [32], implemented in the `statsmodels.api.OLS` funciton in Statsmodel [33].

If the parameters τ_r or τ_d have a significant effect on the neuronal avalanches, then it will have at least partly explain the variance in the power-law coefficient α, which will yield a significant non-zero polynomial term coefficient β_i [34].

IV. Results

A. Tuning the E / I Synaptic Weight Balance

In E-I Networks, tuning the excitatory and inhibitory synaptic weights is critical to achieving a balanced critical network. Too weak synaptic strength and network activity won't propagate; too strong synaptic strength and the network activity falls into a state of overactivity. Figure 5 shows how the network dynamics dramatically change with different synaptic tunings; for the same type of input. For the remainder of this section, the simulations will be performed with $\Delta g_{ex} = 5.0$ and $\Delta g_{inh} = -80.0$.

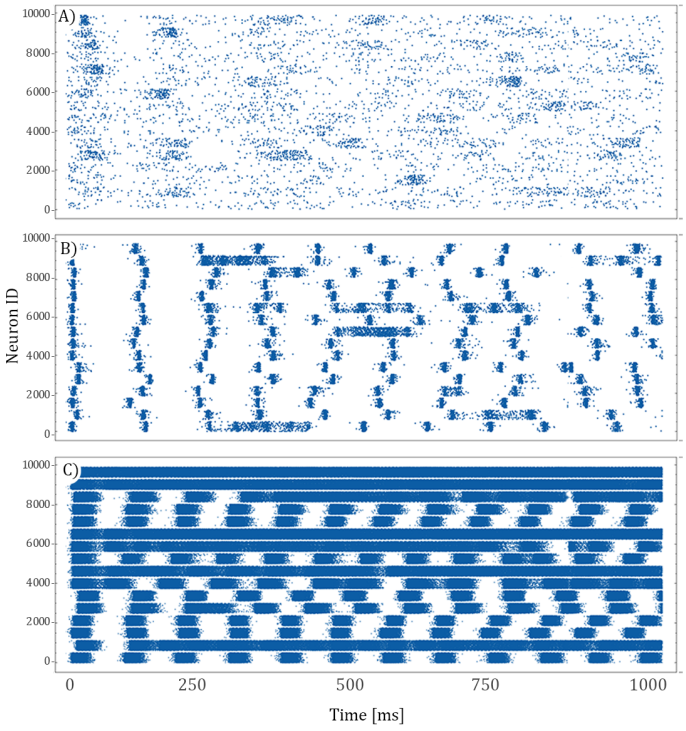

Fig. 5. Spike trains illustrating the dynamics of differently tuned E/I Networks for the same type of input. N=10 000, synaptic delay τ_d = 2.0 ms and neuronal refractory period τ_{ref} = 5.0 ms. (a) $\Delta g_{ex} = 1.0$ and $\Delta g_{inh} = -80.0$: an under-tuned network, where spikes are not able to propagate. (b) $\Delta g_{ex} = 5.0$ and $\Delta g_{inh} = -80.0$: a properly tuned network where spikes are able to propagate. (c) $\Delta g_{ex} = 5.0$ and $\Delta g_{inh} = -17.0$: an over-tuned network, where spikes propagate but bloat the network dynamics.

B. Quantify the neuronal avalanches

In a log-log plot, a power law distribution $y = Cx^a$ becomes a straight line $log(y) = a\ log(x) + log(C)$ with slope a. Figure 6 shows the resulting distributions in a log-log plot after simulating for 4 000 ms with the parameter configuration τ_d = 2.0 ms and τ_{ref} = 5.0 ms.

The avalanche durations result in a line with a downward bending curvature. The avalanche sizes and silent periods also form a straight line for smaller sizes but have an accumulated pile of frequencies for larger sizes.

A possible explanation for the piles is because of the simulation time. Larger avalanches and longer silent periods are increasingly rarer events, meaning that their estimated probability at some point will be truncated as a consequence of a finite simulation time.

C. Estimate the power-law coefficients

We now fit the estimated probability distributions to power-law distributions. Figure 7 and Figure 8 show the resulting power-law exponents β and κ from fitting the probability distributions of avalanche size and avalanche duration, respectively. The standard deviation of each exponent is represented as vertical bars with dots at the end. It is clear that both surfaces look very similar, but are shifted in the z-direction.

Figure 9 shows the resulting exponent after fitting a power-law function to the silent period distribution. This

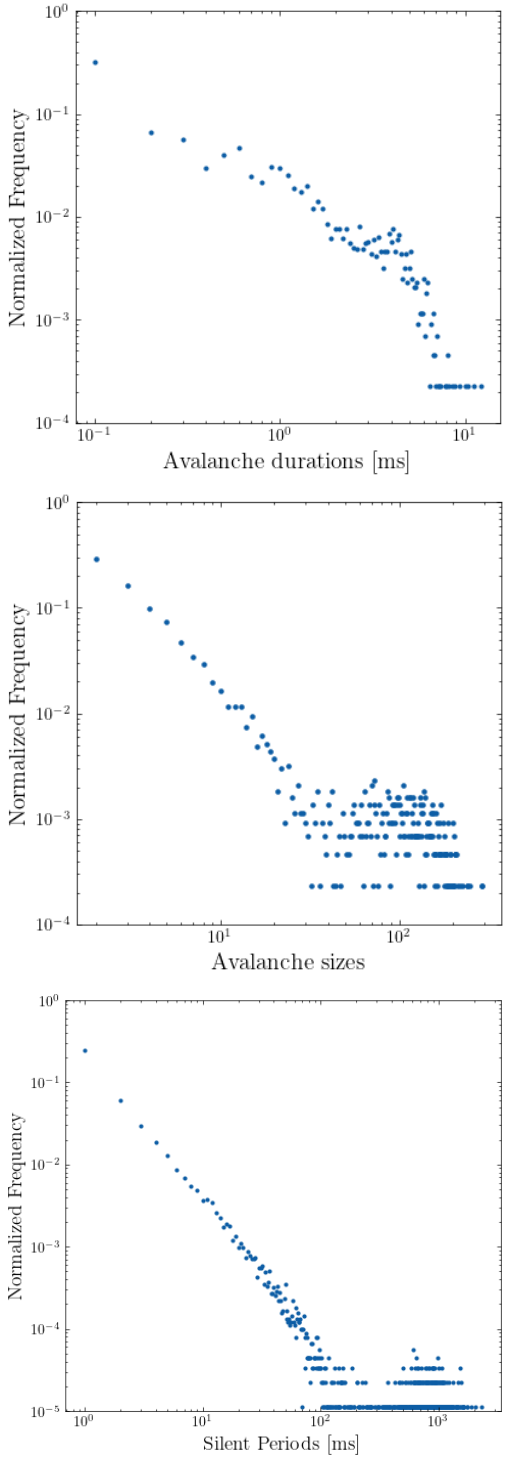

Fig. 6. A log-log plot of the normalized frequency tables with bin size 1 ms for the three avalanche metrics: Duration, Size, and Silent Period. The simulation was run for 4 000 ms with the parameter configuration τ_d = 2.0 ms and τ_{ref} = 5.0 ms.

surface has a different curvature compared to the ones for β and κ. The surface peaks the most for $\tau_r = 1.0$ ms and $\tau_d = 1.0$ ms.

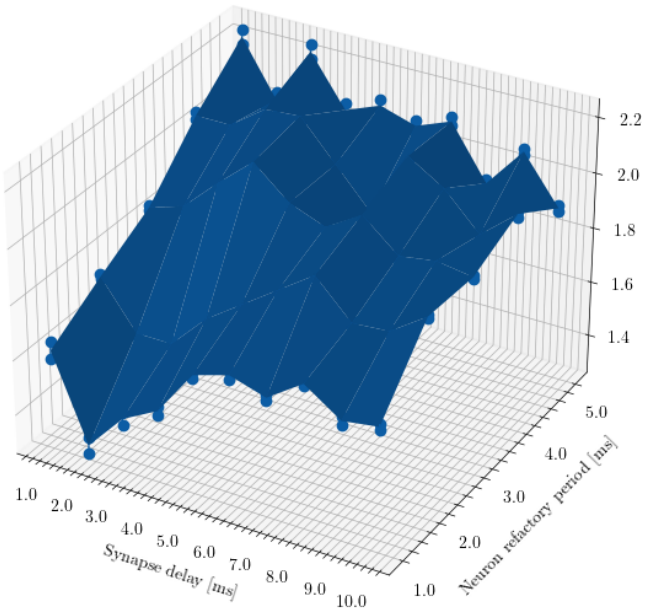

Fig. 7. Avalanche size exponent β as a function of synaptic delay and neuronal refractory time

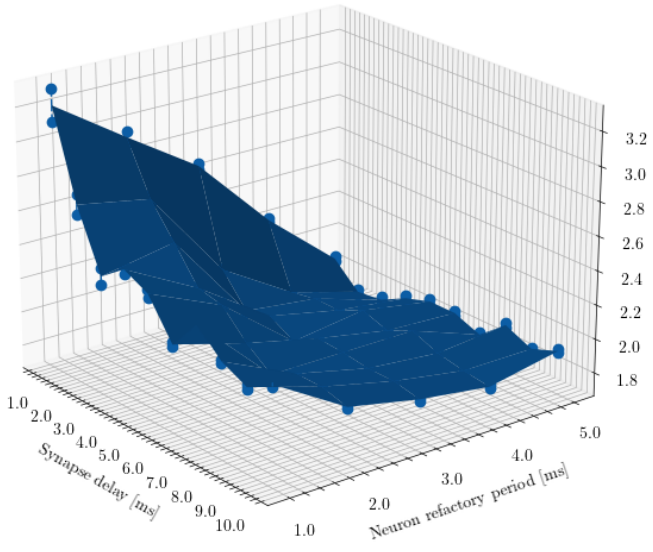

Fig. 9. Silent period l as a function of synaptic delay and neuronal refractory time

Figure 10 shows the result of calculating γ from the avalanche size and duration exponents. The errors were estimated by maximizing and minimizing γ with respect to the errors of β and κ. To compute γ_{max}, we used $\kappa + error(\kappa)$ (since it is in the denominator) and $\beta - error(\beta)$ (since it is in the numerator). γ_{min} were computed analogously.

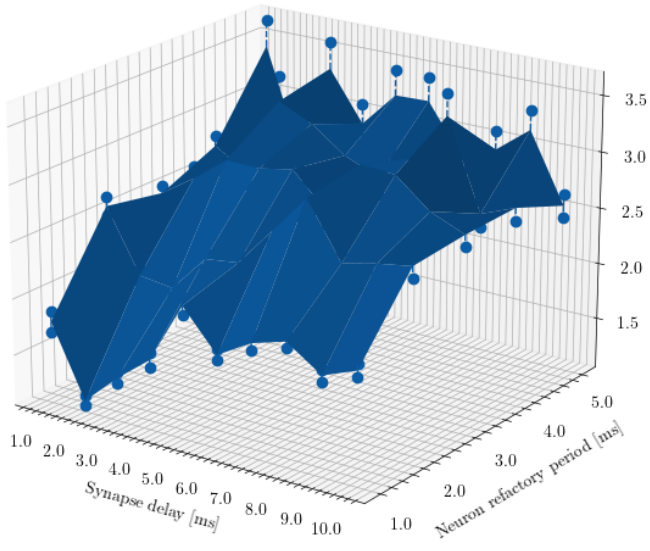

Fig. 8. Avalanche duration exponent κ as a function of synaptic delay and neuronal refractory time

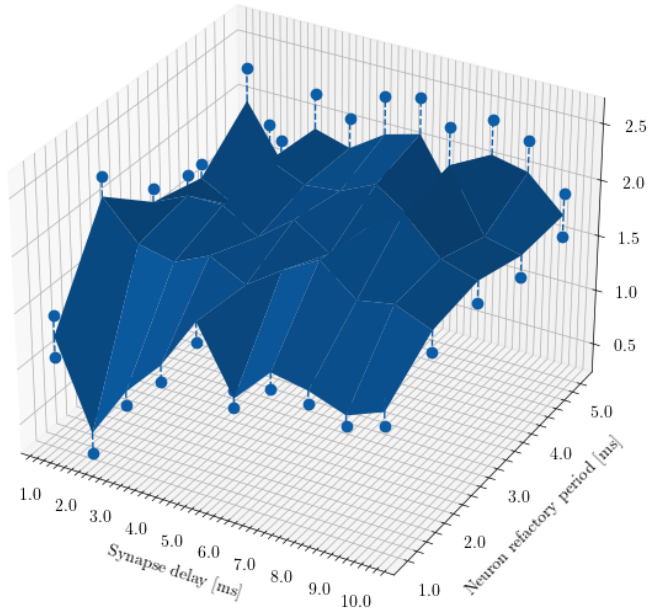

Fig. 10. Criticality factor γ as a function of synaptic delay and neuronal refractory time

D. Quantify the impact of synaptic delay and neuron refractory period

The result of fitting the power-law exponents to the multivariate polynomial in Eq. 10 are presented in the following four tables. The table rows are indexed by their respective independent variable for each parameter $\{\beta_i\}$. The columns *coeff* and *std err* shows the resulting parameter value along with the standard error. To quantify the significance of the parameter, we performed a t-test on each parameter with the null hypothesis $\beta_i = 0$. Column *t* presents the resulting t-test statistic, $P > |t|$ the p-value, followed by two columns showing the 95%-confidence interval. Using a significance of $\alpha = 0.05$, significant p-values have been highlighted in bold. The model adjusted R^2 and resulting F-statistics are shown under the table.

In Table I and Table II, the result of fitting the avalanche size and duration exponents β and κ are presented, respectively. The t-test classifies τ_d, τ_d^2 and the cross-term $\tau_d\tau_r$ as significant in both models. For β, the constant term is also significant while κ has the refractory period parameter τ_r classified as significant.

TABLE I
OLS REGRESSION RESULTS OF FITTING THE AVALANCHE SIZE EXPONENT β

	coef	std err	t	$P > \|t\|$	[0.025	0.975]
const	0.99	0.09	10.76	**0.00**	0.81	1.18
τ_d	0.37	0.05	7.50	**0.00**	0.27	0.47
τ_r	0.08	0.02	3.76	**0.00**	0.04	0.13
τ_d^2	-0.03	0.01	-3.68	**0.00**	-0.04	-0.01
$\tau_d\tau_r$	-0.02	0.00	-5.36	**0.00**	-0.02	-0.01
τ_r^2	-0.00	0.00	-1.30	0.2	-0.01	0.00

$Adj.R^2$ = 0.822, F-statistics: 39.8

TABLE II
OLS REGRESSION RESULTS OF FITTING THE AVALANCHE DURATION EXPONENT κ

	coef	std err	t	$P > \|t\|$	[0.025	0.975]
const	0.26	0.27	0.96	0.34	-0.28	0.80
τ_d	1.03	0.14	7.18	**0.00**	0.74	1.32
τ_r	0.22	0.06	3.40	**0.00**	0.09	0.34
τ_d^2	-0.10	0.02	-4.59	**0.00**	-0.15	-0.06
$\tau_d\tau_r$	-0.03	0.01	-3.04	**0.00**	-0.05	-0.01
τ_r^2	-0.01	0.00	-1.87	0.07	-0.02	0.00

$Adj.R^2$ = 0.747, F-statistics: 29.4

In Table III, the result of fitting the critical exponent γ is presented. The t-test classified τ_d as having a significant impact with degrees 1 and 2. The p-value of τ_r is just on the verge of being significant. Both the adj. R^2 and F-statistic is lower for this model compared to the result for β and κ.

In Table IV, the result of fitting the silent period exponent l is presented. Strikingly, all parameters are classified as significant by the t-test. This result is supported by the fact that the result also has the highest adj. R^2 and F-statistic of all models.

TABLE III
OLS REGRESSION RESULTS OF FITTING γ

	coef	std err	t	$P > \|t\|$	[0.025	0.975]
const	0.38	0.25	1.50	0.14	-0.13	0.88
τ_d	0.69	0.14	5.12	**0.00**	0.42	0.96
τ_r	0.12	0.06	2.03	0.05	0.00	0.24
τ_d^2	-0.09	0.02	-4.28	**0.00**	-0.13	-0.05
$\tau_d\tau_r$	-0.01	0.01	-0.84	0.41	-0.02	0.01
τ_r^2	-0.01	0.00	-1.38	0.17	-0.02	0.00

$Adj.R^2$ = 0.532, F-statistics: 9.7

TABLE IV
OLS REGRESSION RESULTS OF FITTING THE SILENT PERIOD EXPONENT l

	coef	std err	t	$P > \|t\|$	[0.025	0.975]
const	3.71	0.12	29.83	**0.00**	3.46	3.96
τ_d	-0.46	0.07	-6.90	**0.00**	-0.60	-0.33
τ_r	-0.26	0.03	-8.96	**0.00**	-0.32	-0.20
τ_d^2	0.03	0.01	2.51	**0.02**	0.00	0.05
$\tau_d\tau_r$	0.03	0.00	6.51	**0.00**	0.02	0.04
τ_r^2	0.01	0.00	5.24	**0.00**	0.01	0.02

$Adj.R^2$ = 0.858, F-statistics: 59.2

V. DISCUSSION

A. Addressing the impact on neuronal avalanches

Some intuitive feel behind the power-law exponent can be gained by thinking of the log-log plot. A greater absolute value of the exponent implies a steeper downwards slope, which is a result of the distribution being more centered towards smaller values. Looking at the surfaces of avalanche size and duration in Figures 7 and 8, it appears that as both the synaptic delay and the neuron refractory period gets smaller, the power-law exponent decreases in terms of absolute value. This implies that the distribution of avalanche duration and sizes tends to sample greater values. In other words, the avalanches gets both longer and larger in terms of spikes. Applying the same reasoning on the surfaces of silent period l in Figure 9, we can draw the conclusion that the silent periods instead tends to get shorter when the synaptic delay and refractory period decreases.

This intuitive reasoning based on the surfaces, is also supported by the model fitting results. All of the three avalanche metrics (size, distribution and silent period) had very good model fitting results. Their adj. R^2 scores are around 0.8, which can be interpreted as the variables explaining 80% of the variance within the data. In combination with their F-statistics being very high, we can draw the conclusion that the parameters most likely do have a significant impact on the characteristics of neuronal avalanches.

B. Addressing the research questions

To address the our research questions, we must take a step back. Clearly, the synaptic delay and neuronal refractory period have a signifcant impact on neuronal avalanches. That is supported by the results on all of the three avalanche metrics. However, the research question seeked out to investigate if

synaptic delay and neuronal refractory period had a significant impact on criticality in HMN; not on neuronal avalanches.

First, the theory of self-organized criticality predicts a critical system to have $\beta = 2$, $\kappa = 1.5$ and $\gamma = 2$. Looking at the surfaces, both β and κ are off the predicted values for most combinations of synaptic delay and refractory period. However, they manage to stay within just the right ranges in relation to each other to ensure that γ stays relatively close to the predicted value.

Looking at the regressions results in Table III of γ, the results are not as convincing as the other three. Based on the adj R^2, the parameters only explain 50 % of the variance (compared to the previous result of 80 %). While the F-statistic is significant, it has a much less margin of confidence, with only τ_d and τ_d^2 being significant parameters. Somehow, in computing γ the significance of the refractory period vanished.

A possible explanation for this could be attained by recalling that power-law distributed avalanches can occur in random systems that are not critical, but as a result of correlations. And that we can look at the distribution of avalanches shapes (described by γ) to account for this correlation. Then, it could be interpreted that while synaptic delay has a significant impact on *criticality*, neuronal refractory period only affects correlations between avalanche characteristics.

Thus, based on these results, we draw the conclusion that only synaptic delay has a significant impact on network criticality. The type of relation is the sum of a linear and a quadratic term.

C. Addressing the validity and reliability of the results

As mentioned in the results, we observed that some avalanche metrics distributions tended to pile up towards increasingly rarer events as consequence of a finite simulation time. To get more accurate distributions, the simulation time could be increased. If the pile ends up being too big, it could affect the regression and yielding biased results.

One important aspect for the validity of the results is the length of the avalanche step size. In this study, we used an avalanche step size of 1.0 ms, while other studies seems to have used the simulation step size (which is 0.1 ms) [14]. The value of this parameter has a significant impact on the results, since it lays the founding criteria on how to sample the distributions. When we re-ran the study here with an avalanche step size of 0.1 ms, the results results changed.

Finally, it is important to remember that the simulations here was performed with 10 000 neurons, which is a very small sample of the total number of neurons in real cortical brain networks. The important takeaway from this study is therefore primarily on how to setup other simulations of similar sizes with high degree of validity, rather than addressing functionality of real world cortical brain networks.

VI. Conclusion

We studied the impact of synaptic delay and neuronal refractory period on criticality in hierarchical modular neural networks (HMN). The results showed that both variables had a significant impact on the characteristics of neuronal avalanches, which is an phenomena of critical dynamics. However, the analysis indicates the it is only the synaptic delay that has a significant impact on critical dynamics as the impact of neuronal refractory period vanished. To conclude, further studies using HMN to investigate criticality should not overlook the impact synaptic delay has on the results.

References

[1] S. Herculano-Houzel, "The human brain in numbers: a linearly scaled-up primate brain," *Frontiers in human neuroscience*, p. 31, 2009.

[2] P. Bak, *How nature works: the science of self-organized criticality*. Springer Science & Business Media, 2013.

[3] J. M. Beggs and D. Plenz, "Neuronal avalanches in neocortical circuits," *Journal of neuroscience*, vol. 23, no. 35, pp. 11 167–11 177, 2003.

[4] E. D. Gireesh and D. Plenz, "Neuronal avalanches organize as nested theta-and beta/gamma-oscillations during development of cortical layer 2/3," *Proceedings of the National Academy of Sciences*, vol. 105, no. 21, pp. 7576–7581, 2008.

[5] A. Kohn and M. A. Smith, "Utah array extracellular recordings of spontaneous and visually evoked activity from anesthetized macaque primary visual cortex (v1)," *CRCNS. org*, vol. 10, p. K0NC5Z4X, 2016.

[6] K. J. Miller, L. B. Sorensen, J. G. Ojemann, and M. Den Nijs, "Power-law scaling in the brain surface electric potential," *PLoS computational biology*, vol. 5, no. 12, p. e1000609, 2009.

[7] M. Tsodyks, K. Pawelzik, and H. Markram, "Neural networks with dynamic synapses," *Neural computation*, vol. 10, no. 4, pp. 821–835, 1998.

[8] A. Levina, J. M. Herrmann, and T. Geisel, "Dynamical synapses causing self-organized criticality in neural networks," *Nature physics*, vol. 3, no. 12, pp. 857–860, 2007.

[9] B. Del Papa, V. Priesemann, and J. Triesch, "Criticality meets learning: Criticality signatures in a self-organizing recurrent neural network," *PloS one*, vol. 12, no. 5, p. e0178683, 2017.

[10] M. Müller-Linow, C. C. Hilgetag, and M.-T. Hütt, "Organization of excitable dynamics in hierarchical biological networks," *PLoS computational biology*, vol. 4, no. 9, p. e1000190, 2008.

[11] C.-C. Hilgetag, G. A. Burns, M. A. O'Neill, J. W. Scannell, and M. P. Young, "Anatomical connectivity defines the organization of clusters of cortical areas in the macaque and the cat," *Philosophical Transactions of the Royal Society of London. Series B: Biological Sciences*, vol. 355, no. 1393, pp. 91–110, 2000.

[12] H. A. Swadlow, "Physiological properties of individual cerebral axons studied in vivo for as long as one year," *Journal of neurophysiology*, vol. 54, no. 5, pp. 1346–1362, 1985.

[13] M. Rubinov, O. Sporns, J.-P. Thivierge, and M. Breakspear, "Neurobiologically realistic determinants of self-organized criticality in networks of spiking neurons," *PLoS computational biology*, vol. 7, no. 6, p. e1002038, 2011.

[14] S.-J. Wang, C. C. Hilgetag, and C. Zhou, "Sustained activity in hierarchical modular neural networks: self-organized criticality and oscillations," *Frontiers in computational neuroscience*, vol. 5, p. 30, 2011.

[15] S.-J. Wang and C. Zhou, "Hierarchical modular structure enhances the robustness of self-organized criticality in neural networks," *New Journal of Physics*, vol. 14, no. 2, p. 023005, 2012.

[16] W. Gerstner and W. M. Kistler, *Spiking neuron models: Single neurons, populations, plasticity*. Cambridge university press, 2002.

[17] D. Purves, G. J. Augustine, D. Fitzpatrick, L. C. Katz, A.-S. LaMantia, J. O. McNamara, and S. Mark Williams, "Excitatory and inhibitory postsynaptic potentials," *Neuroscience*, pp. 2–3, 2001.

[18] M. Megıas, Z. Emri, T. Freund, and A. Gulyas, "Total number and distribution of inhibitory and excitatory synapses on hippocampal ca1 pyramidal cells," *Neuroscience*, vol. 102, no. 3, pp. 527–540, 2001.

[19] T. P. Vogels and L. F. Abbott, "Signal propagation and logic gating in networks of integrate-and-fire neurons," *Journal of neuroscience*, vol. 25, no. 46, pp. 10 786–10 795, 2005.

[20] A. H. Seidl, "Regulation of conduction time along axons," *Neuroscience*, vol. 276, pp. 126–134, 2014.

[21] A. Maida, "Cognitive computing and neural networks: Reverse engineering the brain," in *Handbook of Statistics*. Elsevier, 2016, vol. 35, pp. 39–78.

[22] D. R. Chialvo, "Emergent complex neural dynamics," *Nature physics*, vol. 6, no. 10, pp. 744–750, 2010.

[23] E. M. Rauch, M. M. Millonas, and D. R. Chialvo, "Pattern formation and functionality in swarm models," *Physics Letters A*, vol. 207, no. 3-4, pp. 185–193, 1995.
[24] B. D. Malamud, G. Morein, and D. L. Turcotte, "Forest fires: an example of self-organized critical behavior," *Science*, vol. 281, no. 5384, pp. 1840–1842, 1998.
[25] T. Lux and M. Marchesi, "Scaling and criticality in a stochastic multi-agent model of a financial market," *Nature*, vol. 397, no. 6719, pp. 498–500, 1999.
[26] T. E. Harris *et al.*, *The theory of branching processes*. Springer Berlin, 1963, vol. 6.
[27] J. Touboul and A. Destexhe, "Power-law statistics and universal scaling in the absence of criticality," *Physical Review E*, vol. 95, no. 1, p. 012413, 2017.
[28] N. Friedman, S. Ito, B. A. Brinkman, M. Shimono, R. L. DeVille, K. A. Dahmen, J. M. Beggs, and T. C. Butler, "Universal critical dynamics in high resolution neuronal avalanche data," *Physical review letters*, vol. 108, no. 20, p. 208102, 2012.
[29] D. Battaglia, N. Brunel, and D. Hansel, "Temporal decorrelation of collective oscillations in neural networks with local inhibition and long-range excitation," *Physical review letters*, vol. 99, no. 23, p. 238106, 2007.
[30] N. Brunel, "Dynamics of networks of randomly connected excitatory and inhibitory spiking neurons," *Journal of Physiology-Paris*, vol. 94, no. 5-6, pp. 445–463, 2000.
[31] P. Virtanen, R. Gommers, T. E. Oliphant, M. Haberland, T. Reddy, D. Cournapeau, E. Burovski, P. Peterson, W. Weckesser, J. Bright, S. J. van der Walt, M. Brett, J. Wilson, K. J. Millman, N. Mayorov, A. R. J. Nelson, E. Jones, R. Kern, E. Larson, C. J. Carey, İ. Polat, Y. Feng, E. W. Moore, J. VanderPlas, D. Laxalde, J. Perktold, R. Cimrman, I. Henriksen, E. A. Quintero, C. R. Harris, A. M. Archibald, A. H. Ribeiro, F. Pedregosa, P. van Mulbregt, and SciPy 1.0 Contributors, "SciPy 1.0: Fundamental Algorithms for Scientific Computing in Python," *Nature Methods*, vol. 17, pp. 261–272, 2020.
[32] X. Su, X. Yan, and C.-L. Tsai, "Linear regression," *Wiley Interdisciplinary Reviews: Computational Statistics*, vol. 4, no. 3, pp. 275–294, 2012.
[33] S. Seabold and J. Perktold, "statsmodels: Econometric and statistical modeling with python," in *9th Python in Science Conference*, 2010.
[34] J. Gareth, W. Daniela, H. Trevor, and T. Robert, *An introduction to statistical learning: with applications in R*. Spinger, 2013.